Weather and Climate Dynamics

Supercell convective environments in Spain based on ERA5: hail and non-hail differences

Carlos Calvo-Sancho[1], Javier Díaz-Fernández[2], Yago Martín[3], Pedro Bolgiani[2], Mariano Sastre[2], Juan Jesús González-Alemán[4], Daniel Santos-Muñoz[5], José Ignacio Farrán[1], and María Luisa Martín[1,6]

[1]Department of Applied Mathematics, Faculty of Computer Engineering, University of Valladolid, Segovia, Spain
[2]Department of Earth Physics and Astrophysics, Faculty of Physics, Complutense University of Madrid, Madrid, Spain
[3]Department of Geography, Faculty of History and Philosophy, University Pablo de Olavide, Seville, Spain
[4]State Meteorological Agency (AEMET), Madrid, Spain
[5]Department of Research and Development, Danmarks Meteorologiske Institut, Copenhaguen, Denmark
[6]Institute of Interdisciplinary Mathematics (IMI), Complutense University of Madrid, Madrid, Spain

Correspondence: Carlos Calvo-Sancho (carlos.calvo.sancho@uva.es)

Abstract. Severe convective storms, in particular supercells, are occasionally responsible for a large number of property losses and damage in Spain. This paper aims to study the synoptic configurations and pre-convective environments in a dataset of 262 supercells during 2011–2020 in Spain. The events are grouped into supercells with hail (diameter larger than 5 cm) and without hail and the results are compared. ERA5 reanalysis is used to study the synoptic configurations and proximity atmospheric profiles related to the supercell events at the initial time. In addition, temperature, convective available potential energy, convective inhibition, lifting condensation level, level of free convection, height of freezing level, wind shear and storm-relative helicity are obtained for each event. Results show that supercells are more frequent on the Mediterranean coast during the warm season. Some of the variables analyzed present statistically significant differences between hail and non-hail events. In particular, supercells with hail are characterized by higher median values of most-unstable convective available potential energy than supercells without hail.

1 Introduction

Thunderstorms and their associated phenomena (lightning, hail, wind or flash floods) have a great influence on human activities due to their destructive consequences (Martín et al., 2020; Taszarek et al., 2020a; Rodriguez and Bech, 2021). Europe is regularly threatened by severe thunderstorms (Dahl, 2006), causing considerable economic loss, having a social impact, and endangering aviation safety (Nisi et al., 2016; Mohr et al., 2017; Antonescu et al., 2017; Kunz et al., 2020; Chernokulsky et al., 2020; Gatzen et al., 2020). Thus, improving the knowledge on the genesis and life cycle of thunderstorms is a constant endeavor in the meteorological community.

Thunderstorm cells can be formed either in a discrete and isolated form or in large and organized systems, (e.g., squall lines). Three different thunderstorm types are defined by the US National Weather Service (NWS, 2019) based on their structure, organization and size: ordinary cell, multicell and supercell. Browning (1962) defines supercells as thunderstorms occurring in a significantly vertically sheared environment, which contains a deep and persistent mesocyclone, representing the most organized, severe and long-lasting form of isolated deep convection phenomena. These systems are linked to hail reports – including hail diameters larger than 5 cm – and EF2 tornadoes or higher (Duda and Gallus, 2010; Quirantes et al., 2014; Blair et al., 2017). Supercells are common phenomena in spring and summer (Brooks et al., 2019), and can be detected through Doppler radar data to confirm the associated mesocyclone (Blair et al., 2011; Kahraman et al., 2017). Moreover, ground-based or satellite lightning detection systems can be useful as support-

ing information (Bedka et al., 2018; Galanaki et al., 2018). However, local phenomena associated with these systems, such as hail, require observational reports to be confirmed. Since many of these events occur in unpopulated areas, the observed weather reports have a spatial bias toward the most populated areas (Groenemeijer et al., 2017; Edwards et al., 2018). In recent years, thunderstorm and severe weather reports have increased due to the accessibility of the general population to new technologies, especially thanks to smart phones and social networks. This has enabled an improvement in databases related to thunderstorms and their effects, with increasing availability of information on these events (Elmore et al., 2014; Krennert et al., 2018; Taszarek et al., 2020b). Nevertheless, a rigorous quality and validity control, through validated observational data (radar, satellite, etc.), should be applied for these severe-weather reports to be scientifically valid (Dotzek et al., 2009).

Mainly due to orography, lower convective available potential energy (CAPE) and wind shear (WS), supercells in Europe tend to be less severe – return periods of hail $\geq 8\,\mathrm{cm}$ or violent tornadoes are longer than those formed in the United States. Thus, supercells in Europe tend to show lower rotation velocities and shorter life spans (Quirantes et al., 2014; Taszarek et al., 2020b). The study of severe convective storms in Spain has increased in recent years, extending the knowledge about these systems in the country. Martín et al. (2020) found more than 100 supercells per year on average in Spain. Weather environments conducive to severe convective storms have been identified in different studies suggesting that synoptic environments (Merino et al., 2013; Mora et al., 2015), mesoscale characteristics (García-Ortega et al., 2012), orography (Romero et al., 1998) and convective variables (Calvo-Sancho and Martín, 2021) should be considered together in the research of supercells. In this sense, Castro et al. (1992) explored the role of topography in the formation and evolution of thunderstorms in the Ebro Valley (Fig. 1), concluding that mountainous terrain affects the trajectories and velocities of supercells. Regarding hailstorms, Merino et al. (2013) highlight that the main triggers of convection are thermal instability and low-level convergence. The occurrence and intensity of tornadoes are not as severe or frequent as in other regions of the world (e.g., the United States) mainly due to the absence of wet fluxes inland (Rodríguez and Bech, 2018). However, the occurrence of these events in northeastern Spain has caused substantial damage for the local economy, especially in crop fields (López and Sanchez, 2009). Gayà (2011) performed a climatology study of tornadoes and waterspouts in Spain and Rodríguez and Bech (2018, 2021) surveyed the mesoscale environments wherein tornadoes and waterspouts formed in the Iberian Peninsula. Both studies reveal that WS plays a more important role than CAPE in synoptic and mesoscale environments in the cold season.

Since severe supercells have caused substantial property damage and economic losses in recent years in Spain, with around 300 casualties due to thunderstorms from 1987 to 2020 (Consorcio de Compensación de Seguros, 2020), this study aims to provide a better understanding of the supercell synoptic and mesoscale environments. To this end, a set of events are selected from the supercell database of Martín et al. (2020), which are then categorized into two distinct groups, i.e., with hail diameter larger than 5 cm (SP-HAIL) and without hail (SP-NONHAIL). Manzato (2012) recorded hailstorms using hailpads to perform a hail climatology analysis in northeast Italy. Merino et al. (2013) also used hailpads data to study the synoptic and mesoscale configurations for hailstorms in southwestern Europe.

Herein, these systems are analyzed through their synoptic and mesoscale environments using ERA5 reanalysis (Hersbach et al., 2020). ERA5 is a state-of-the-art, high-resolution reanalysis, which has yielded successful results in studies related to severe local thunderstorm environments over North America (Coffer et al., 2020; Li et al., 2020; Taszarek et al., 2020a, b) and Europe (Taszarek et al., 2020a, b; Calvo-Sancho and Martín, 2021), to tornadic environments in the Iberian Peninsula (Rodríguez and Bech, 2021), and to microbursts (Bolgiani et al., 2020). On the other hand, severe storms have been forecast using numerical weather prediction models and alternative methods based on them, as seen in Gascón et al. (2015) survey. Their study selected the Showalter Index, dew point temperature at 850 hPa, storm relative helicity between 0 and 3 km, wind speed at 500 hPa and wet bulb zero to develop a logistic equation that generated the probability of severe thunderstorm development, obtaining a robust instrument to forecast severe thunderstorms in the Ebro Valley region.

This work is organized as follows. The database and methodology are described in Sect. 2. Section 3 presents the discussion of the main results related to synoptic and convective variables associated with SP-HAIL and SP-NONHAIL events. Finally, the main conclusions are summarized in Sect. 4.

2 Data and methodology

2.1 Datasets

The supercell sample used is selected from the Spanish Supercell Database (Martín et al., 2020) for the period 2011–2020. This dataset is formed by confirmed (i.e., Doppler radar images, hail greater than 5 cm reports, tornadoes greater than EF2 or images of the event) and medium–high confidence (detected in non-Doppler radar images but without direct observation; see Fig. 4 in Martín et al., 2020) supercell events through reports from volunteers and collaborators. This dataset comprises a total of 1758 supercells, of which 262 correspond to confirmed supercells and 1495 to medium–high confidence supercells. It is worth noting that even though the database covers all of Spain's national terri-
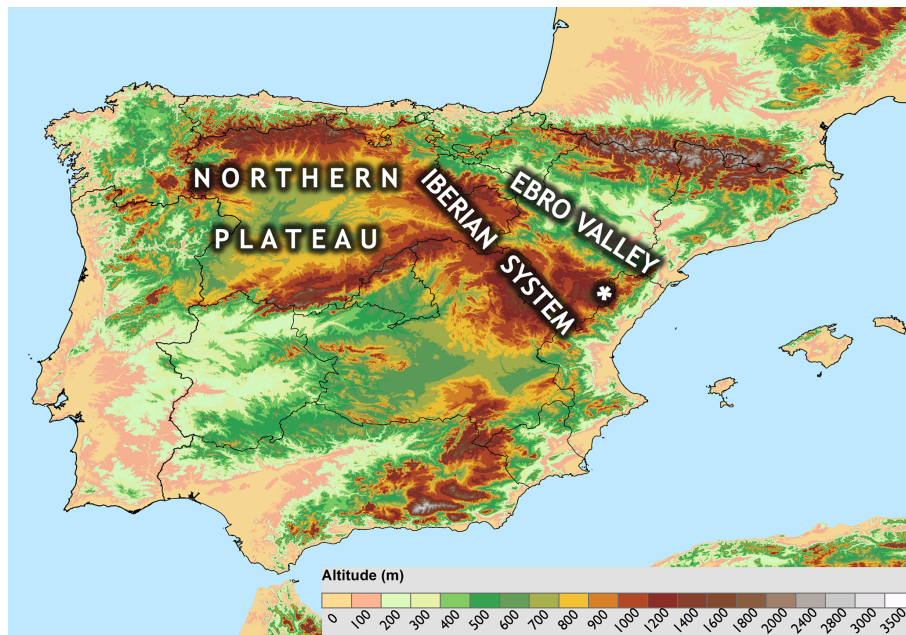
Figure 1. Domain and orography of the study area (m). White star indicates Maestrazgo area.

tory, there are no events reported in the Canary Islands. The database defines the supercell spatial life cycle through an ellipse in a Geographical Information System and collects additional information associated with the events, e.g., hail diameter, tornado intensity. In the current study, only the confirmed supercells are selected. These are then categorized as SP-HAIL and SP-NONHAIL according to the observation of hailstones with a diameter larger than 5 cm or the lack of these reports. It should be noted that in this study the Spanish Supercell Database was cross-matched with the European Severe Weather Database (ESWD) and Notification System for Singular Atmospheric Observations (SINOBAS). The validation results show that more than 80 % of the SP-HAIL events from the Spanish Supercell Database are included in the ESWD and SINOBAS datasets. Finally, the initial formation time (t_0) of each supercell is selected to characterize the development phase of the cell, because once convection is triggered, the environment might be "contaminated" and the variables may not represent the conditions in which the supercell developed.

The ERA5 reanalysis (Hersbach et al., 2020) is selected for the study of the synoptic characteristics and the convective variables involved in the supercell development. This is the fifth generation reanalysis created by the European Centre for Medium-Range Weather Forecasts (ECMWF). It is provided with a horizontal grid resolution of $0.25° \times 0.25°$, 1 h as temporal resolution and 137 hybrid model levels for the vertical resolution, from 1000 to 1 hPa, approximately. In the current work, the domain is delimited to $60/20° \, N \times 30° \, W/30° \, E$ to study the environments related to the supercells in Spain. To analyze the mesoscale set-

ting, a vertical profile of temperature, dew point, geopotential height, pressure, and wind components (u, v) is derived from the ERA5 grid for each supercell event.

2.2 Compositing

Following the methodology of Calvo-Sancho and Martín (2021) and Gensini et al. (2021), supercell soundings for SP-HAIL and SP-NONHAIL events are built for t_0. Each vertical profile is computed from ERA5 using the nearest grid point to the supercell location at t_0. A quality control is carried out to remove any sounding related to convective boundary propagation (Brooks et al., 2003, 2007; Gensini et al., 2021). Accordingly, each vertical profile must record a non-zero most-unstable convective available potential energy (MUCAPE) and mixed-layer level of free convection (MLLFC) to be included in the study. Once the vertical profiles are obtained, composites for SP-HAIL and SP-NONHAIL are derived at t_0.

Synoptic pattern composites of both types of events are created to describe and compare the common large-scale features. The ERA5 atmospheric fields used to compute the composites are 500 and 300 hPa geopotential height, mean sea level pressure, dew point, wind direction and wind speed at 10 meter above sea level, 700–400 hPa integrated mean of omega vertical velocity, and 0–6 km WS. These atmospheric variables have been used in studies related to spatial patterns of hailstorms (Merino et al., 2013; Melcón et al., 2017), supercells (Gropp and Davenport, 2018) and other types of thunderstorms (Mora et al., 2015).

2.3 Convective variables

To characterize the convective environment, several thermo-dynamic and kinematic variables are calculated using the thundeR R language package (Taszarek et al., 2021) for each vertical profile. The selection of these parameters (Table 1) is based on similar studies related to severe convective storms in the United States and Europe (Rasmussen and Blanchard, 1998; Kaltenböck et al., 2009; Westermayer et al., 2016; Rodríguez and Bech, 2018, 2021; Taszarek et al., 2020a; Davenport, 2021). The 2 m temperature (T2M) and dew point (DWPT) are selected. CAPE and convective inhibition (CIN) using most-unstable (MU), mixed-layer (ML; averaged over 0–500 m above ground level) and surface-based (SB) parcels are calculated using the virtual temperature correction (Doswell and Rasmussen, 1994). The deep-layer bulk WS over 0–6 km (WS06) and the effective bulk wind difference (EBWD; limited to the layer in which $CAPE \geq 100\,J\,kg^{-1}$ and $CIN \geq -250\,J\,kg^{-1}$; Thompson et al., 2007) are also calculated. Finally, other parameters relevant to SP-HAIL are also included: ML lifting condensation level (MLLCL), ML level of free convection (MLLFC), height of freezing level (FZH) and height of wet-bulb freezing level (FZH_W).

The application of the non-parametric Mann–Whitney test (Mann and Whitney, 1947) is used to establish statistical differences (at $p < 0.05$) between the SP-HAIL and SP-NONHAIL groups for the aforementioned parameters at t_0 (Table 2). The results show differences for both thermo-dynamic variables, all the CAPE variables and the freezing-level-related variables. Also, MLCIN and EBWD are statistically different.

3 Results and discussion

The spatial and temporal distribution of supercells for both SP-HAIL and SP-NONHAIL formed in the Spanish mainland are first assessed. The main results relative to large-scale composites, and the thermodynamic and kinematic variables involved in supercell formation in the domain, are presented and discussed in the following two subsections.

The spatial distribution of the reported supercell episodes (Fig. 2a) shows that most of the events for both SP-HAIL and SP-NONHAIL took place in the eastern half of Spain. The Ebro Valley and the Mediterranean coastal area accumulate 79.9 % of the SP-NONHAIL and 88.3 % of SP-HAIL. This is consistent with lightning observations in Spain, as the eastern Iberian System area (white star in Fig. 1) has the highest density of lightning flash per year (Mora et al., 2015). This area favors convective initiation and supercell formation due to low-level convergence (northwesterly–southeasterly and south westerly–easterly winds), upper-level forcing for ascent, low–medium-level moist convection coming from the

Mediterranean Sea and strong diurnal heating (Mora et al., 2015).

The temporal distribution of supercell events (Fig. 2b) matches the warmest and stronger insolation months (July and August accumulate 53.3 % of the SP-NONHAIL and 74.4 % of the SP-HAIL storms) in the study area, since deep convection is a necessary condition for the formation of supercells (Markowski and Richardson, 2011; Miglietta et al., 2017; Taszarek et al., 2019). This is consistent with other studies on convective storms in Europe that assess the higher thunderstorm frequency in summertime, when the diurnal heating is stronger (Merino et al., 2013; Kotroni and Lagouvardos, 2016; Taszarek et al., 2018, 2019). The hourly distribution of the supercells (Fig. 2c) shows a concentration of the events during the late afternoon (summer local time is co-ordinated universal time plus 2 h, UTC+2), shortly after the daily insolation maximum in the study area. However, the results also show a large persistence of the conditions, as many events are reported well into the evening.

3.1 Large-scale setting synoptic features

Synoptic pattern composites for the most relevant atmospheric variables in SP-HAIL and SP-NONHAIL events are presented in this subsection to describe and compare the large-scale characteristics.

Non-substantial differences between SP-HAIL and SP-NONHAIL are found in the mean sea level pressure (Fig. 3). However, the 500 hPa geopotential height displays a SP-NONHAIL composite with a deeper trough and weaker geopotential height gradient in comparison with SP-HAIL. A similar situation is shown by the 300 hPa geopotential height. This atmospheric configuration promotes weak WS in upper levels, which could be indicative of weaker convective environments (Weisman and Klemp, 1982; Brooks et al., 2003; Taszarek et al., 2017). Although there are differences between SP-HAIL and SP-NONHAIL, both geopotential configurations promote upper-level positive vorticity advection (not shown) and divergence over Spain, which favor a stronger upper-level forcing (Markowski and Richardson, 2011). Values of $1.1\,Pa^{-1}\,s^{-3}$ in SP-HAIL events at 700–400 hPa thickness of Q-vector divergence (Fig. S1b in the Supplement) and statistical differences of Q-vector divergence between SP-HAIL and SP-NONHAIL events (Fig. S1) are found over eastern Spain. The positive Q-vector divergence values indicate forcing for ascent where supercells could have originated from strong convection. Thermal lows (1012 hPa) can also be appreciated in the center of Spain (Fig. 3b). These lows are typical of the summer months (Tullot, 2000), promoting east wind flows and ensuring humidity from the Mediterranean Sea in the supercell formation area favoring the initiation of deep convection. Thus, a more favorable environment for deep moist convection should be expected for SP-HAIL, as the corresponding composite shows
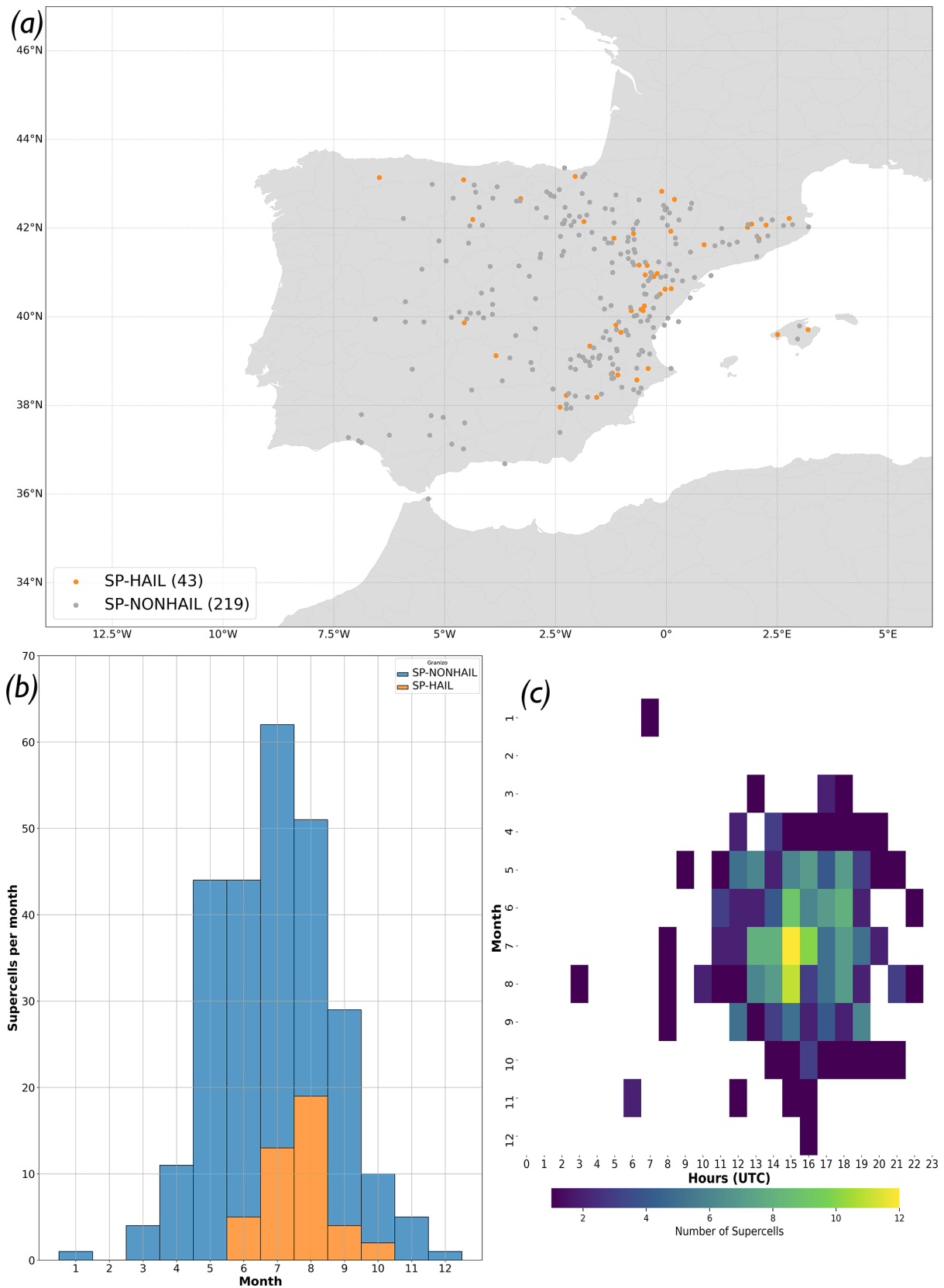
Figure 2. (a) Location of the dataset events (SP-HAIL and SP-NONHAIL) from 2011 to 2020 in Spain. **(b)** Monthly supercell distribution. **(c)** Hourly supercell distribution (t_0; UTC).

Table 1. Description of the convective variables.

Parameter	Abbreviation	Units
Thermodynamic parameters		
2 m Temperature	T2M	°C
2 m Dew-point temperature	DWPT	°C
Parcel parameters		
Most-unstable convective available potential energy	MUCAPE	$J\,kg^{-1}$
Surface-based convective available potential energy	SBCAPE	$J\,kg^{-1}$
Mixed-layer convective available potential energy	MLCAPE	$J\,kg^{-1}$
Most-unstable convective inhibition	MUCIN	$J\,kg^{-1}$
Surface-based convective inhibition	SBCIN	$J\,kg^{-1}$
Mixed-layer convective inhibition	MLCIN	$J\,kg^{-1}$
Mixed-layer lifting condensation level	MLLCL	m
Mixed-layer level of free convection	MLLFC	m
Height of freezing level	FZH	m
Height of wet-bulb freezing level	FZH_W	m
Kinematic parameters		
Deep-layer bulk wind shear over 0–6 km	WS06	$m\,s^{-1}$
Effective bulk wind difference	EBWD	$m\,s^{-1}$
Storm-relative helicity over 0–1 km	SRH01	$m^2\,s^{-2}$
Storm-relative helicity over 0–3 km	SRH03	$m^2\,s^{-2}$
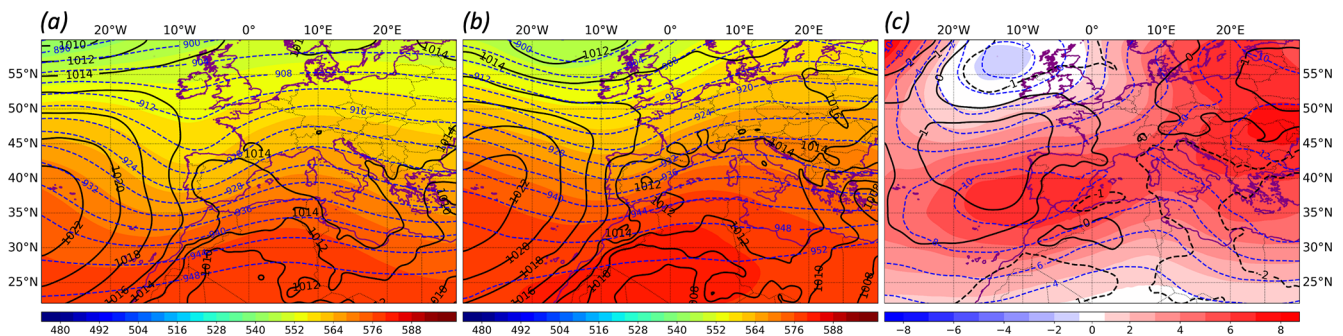
Figure 3. The 500 hPa geopotential height (colored; dam), 300 hPa geopotential height (blue contours; dam) and mean sea level pressure (black lines; hPa) composites at t_0 for **(a)** SP-NONHAIL, **(b)** SP-HAIL and **(c)** differences between SP-HAIL and SP-NONHAIL.

a deeper thermal low, covering a larger area and accompanied by an enhanced easterly flow.

Mora et al. (2015) studied electrical thunderstorms in the northern plateau of Spain during 2000–2010, finding that 31 % of these thunderstorm episodes were linked to upper-level troughs. These episodes were characterized by strong baroclinic short waves and deep troughs at 500 hPa, which is a pattern very similar to the one shown in SP-HAIL and SP-NONHAIL composites in Fig. 3, respectively. Therefore, the results are in line with those of Mora et al. (2015), showing that supercell episodes in Spain are associated with troughs at upper and medium levels of the troposphere. Overall, the higher convective activity is located in the eastern part of

Spain, corresponding to the right side of the troughs, with the thermal lows at the center of Spain.

One of the main features favoring deep moist convection is the moisture at lower and medium levels (Taszarek et al., 2019). Figure 4c depicts statistically significant differences in the DWPT values between SP-HAIL and SP-NONHAIL, with these differences being clearly stronger on the Spanish Mediterranean coast. Inland, a notable difference in DWPT is seen for SP-HAIL over the Ebro Valley (Fig. 4b), along with a stronger easterly wind flow. This would be a consequence of the geopotential and thermal low configuration described earlier, which induces humid air advection from the Mediterranean Sea. According to the DWPT climatology (not shown), the DWPT in the Ebro Valley and the Mediter-
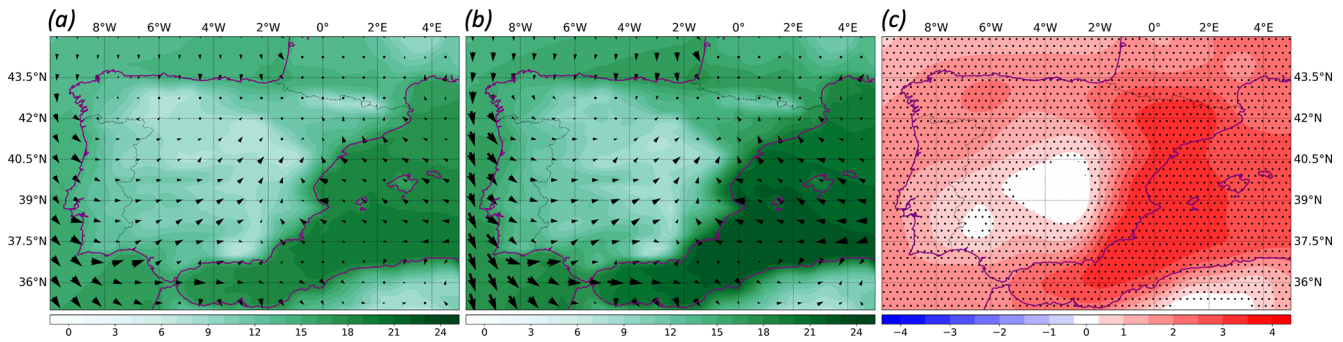
Figure 4. The 2 m dew point temperature (contours; °C) and 10 m wind (arrows; m s^{-1}) composites at t_0 for **(a)** SP-NONHAIL, **(b)** SP-HAIL and **(c)** differences between SP-HAIL and SP-NONHAIL. Black points in panel **(c)** denote statistically significant differences ($p < 0.05$) in dew point temperature.

Table 2. Mann–Whitney test results of all variables analyzed for SP-HAIL and SP-NONHAIL events at t_0 (p values equal to or less than 0.05 are in bold).

	SP-HAIL SP-NONHAIL		SP-HAIL SP-NONHAIL
MUCAPE	**0.00**	MLLFC	0.43
SBCAPE	**0.00**	FZH	**0.00**
MLCAPE	**0.00**	FZH_W	**0.00**
T2M	**0.02**	WS06	0.23
DWPT	**0.00**	WS01	0.17
SBCIN	0.24	EBWD	**0.00**
MLCIN	**0.01**	SRH01	0.44
MUCIN	0.48	SRH03	0.62
MLLCL	0.16		

ranean coast is higher in August (when SP-HAIL is predominant; Fig. 2b) than in July. The convective processes are then supported by the favorable environment that promotes deep convection in those zones and are pushed by the south-westerly flows. This process is consistent with the results of the supercell observations for the period 2011–2020 (Fig. 2a).

The omega vertical velocity composites show statistically significant differences between SP-HAIL and SP-NONHAIL at t_0 (Fig. 5). The omega maxima for both supercell groups throughout the life cycle of the systems are located in the Ebro Valley axis and the Iberian System mountains, where supercells are most common (Fig. 5b). The maxima omega vertical velocity at 700–400 hPa thickness for SP-NONHAIL is larger than for SP-HAIL, except in the Ebro Valley. These higher SP-HAIL omega vertical velocities along with the low-level wind convergence favor convection initiation (Markowski and Richardson, 2011). Therefore, sustained omega vertical velocities (Fig. 5b) and wind convergence (Fig. 4b) trigger, enhance and reinforce deep moist convection at t_0, favoring large hail formation over the Ebro Valley and the Mediterranean area (Gutierrez and Kumjian, 2021).

Vertical WS promotes thunderstorm organization and its longevity. However, excessive WS can be unfavorable to weak updrafts in environments of low instability and, furthermore, can be disadvantageous to convection initiation by increasing entrainment (Markowski and Richardson, 2011). Figure 5 shows similar strong WS06 values (> 20 m s^{-1}) for both SP-HAIL and SP-NONHAIL events. The conjunction of upper-level forcing (Fig. 3), low-level convergence (Fig. 4) and strong omega vertical velocity (Fig. 5) promotes organization, longevity and severity in thunderstorms. Additionally, as depicted in Fig. S1, the maxima Q-vector divergence area (1.1 Pa^{-1} s^{-3}; Fig. S1b) matches with the convergence of Q vectors. Figure S1 shows how the upper-level forcing for ascent is higher in SP-HAIL than SP-NONHAIL events on the Mediterranean coast.

3.2 Convective variables

As described in the convective variables methodology (Sect. 2.3), results of the T2M, DWPT, CAPE, CIN, MLLCL, MLLFC, FZH and WS variables from the ERA5 database are presented in this subsection. These results are shown as violin plots, where the probability density distributions of each variable can be seen as well as the differences between SP-HAIL and SP-NONHAIL events at t_0.

Based on the synoptic compositing methodology, schematic SP-HAIL and SP-NONHAIL composite soundings at t_0 are determined (Fig. 6). In order to show the vertical profile of the supercells developing in highly unstable environments, the 90th percentile (based on MUCAPE values) of the Spanish Supercell Database is selected. The 90th percentile vertical profile for each supercell classification reveals interesting features, particularly on the surface, low levels, and the convective energy. The composite sounding for SP-HAIL (Fig. 6b) displays a larger CAPE area than for SP-NONHAIL (Fig. 6a). This high value of CAPE (1485.9 J kg^{-1}) is strongly associated with vertical accelerations (Markowski and Richardson, 2011), and thus hail formation would be favored. Regarding the CIN, it is
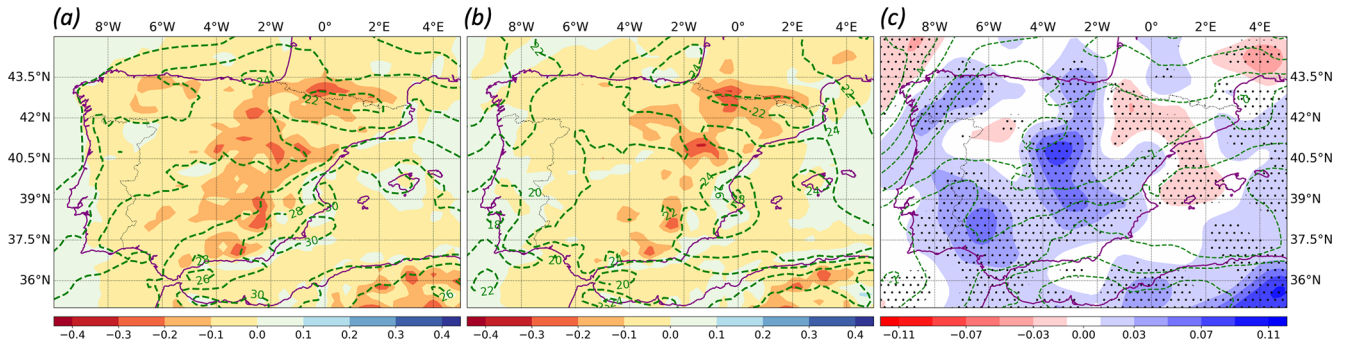
Figure 5. The 700–400 hPa omega vertical velocity (contours; $Pa\,s^{-1}$), 0–6 km WS (green lines; $m\,s^{-1}$) composites at t_0 for **(a)** SP-NONHAIL, **(b)** SP-HAIL and **(c)** differences between SP-HAIL and SP-NONHAIL. Black points in panel **(c)** denote statistically significant differences ($p < 0.05$) in omega vertical velocity.
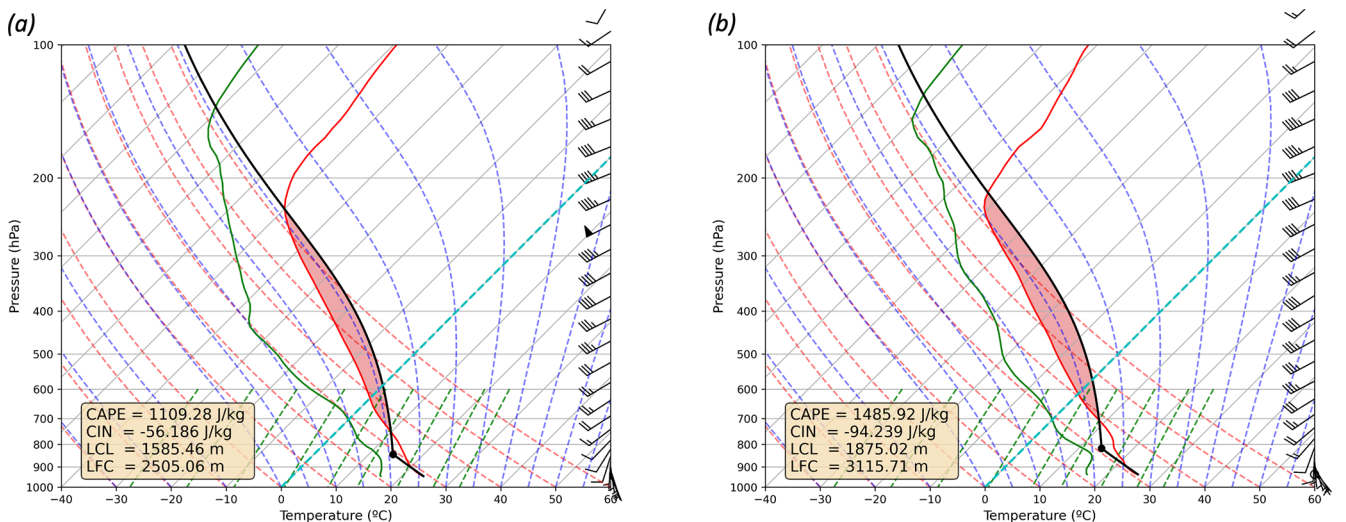

Figure 6. The 90th percentile (based on MUCAPE values) composite soundings at t_0 for **(a)** SP-NONHAIL and **(b)** SP-HAIL. Black dot indicates the LCL value.

higher for SP-HAIL ($-94.2\,J\,kg^{-1}$) than for SP-NONHAIL ($-56.2\,J\,kg^{-1}$). Differences between LCL (Fig. 6, black dot in panels) and LFC are shown, being higher for SP-HAIL than for SP-NONHAIL events. According to Mulholland et al. (2021), a higher LCL is related to the deep convective updraft width. This results in a wider and deeper column and a faster vertical velocity due to the larger distance and residence time of the dry thermal entrainment. The wind barbs reveal a moderate WS06 for both types of supercells. According to Markowski and Richardson (2011) WS tends to enhance the organization, severity and longevity of the deep moist convection. However, SP-HAIL low-level WS is higher than for SP-NONHAIL, favoring hail growth (Gutierrez and Kumjian, 2021).

The distribution for T2M and DWPT shows differences between both types of events, which are statistically significant (Table 2) for both variables. Different distributions can be seen in Fig. 7. The T2M for the SP-HAIL distribution de-

picts a lower variability and larger median value (Table 3) than the corresponding SP-NONHAIL. The T2M maximum (minimum) for SP-HAIL is 33.0 °C (16.8 °C), with both groups showing a very similar maximum value, while the minimum is significantly lower (7.9 °C) for SP-NONHAIL. The DWPT median value for SP-HAIL is greater than for SP-NONHAIL (Table 3). These differences mainly originate from wind flows, since in the Spanish Mediterranean area and the Balearic Islands the main contributor to low-level moisture is advection from the warm Mediterranean Sea. However, in the Spanish inland the main contributor would be the evapotranspiration of the crop fields and vegetation (Vicente-Serrano et al., 2014; Tomas-Burguera et al., 2021), contributing considerably less humidity to the environment.

CAPE is a common and useful forecast tool, in combination with vertical WS, for predicting supercells and hail (Kaltenböck et al., 2009; Merino et al., 2013). The distributions in the parcel measurements of MUCAPE, SBCAPE
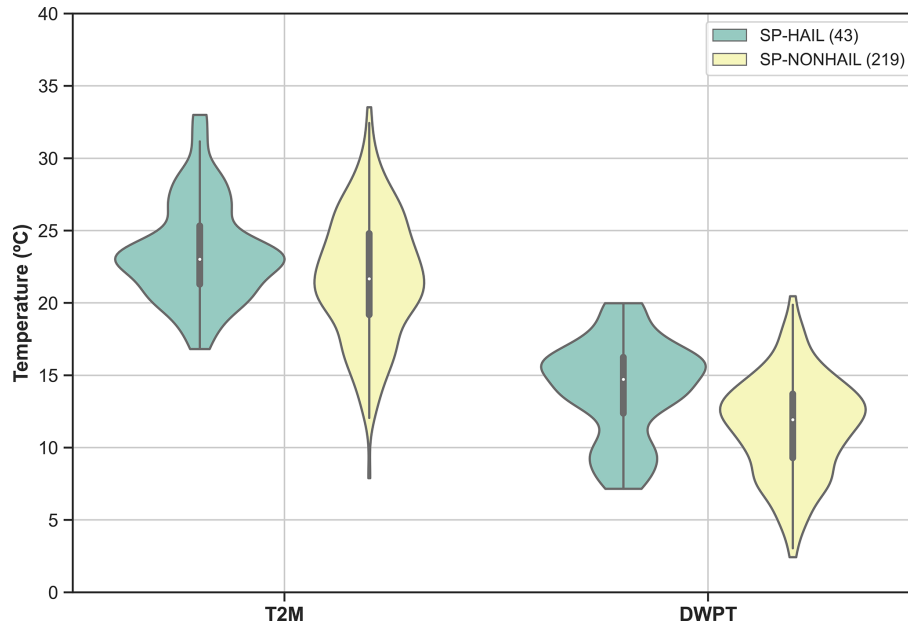
Figure 7. T2M and DWPT distributions and boxplots for SP-HAIL and SP-NONHAIL at t_0. Median values are represented by white points.

Table 3. Median values for each parameter analyzed for SP-HAIL and SP-NONHAIL events at t_c.

	SP-HAIL t_0	SP-NONHAIL t_0
MUCAPE ($J\,kg^{-1}$)	1231.0	691.7
SBCAPE ($J\,kg^{-1}$)	1231.0	662.1
MLCAPE ($J\,kg^{-1}$)	966.1	444.6
T2M (°C)	23.0	21.7
DWPT (°C)	14.7	11.9
SBCIN ($J\,kg^{-1}$)	−5.3	−3.7
MLCIN ($J\,kg^{-1}$)	−20.2	−12.2
MUCIN ($J\,kg^{-1}$)	−3.5	−3.6
MLLCL (m)	1075.0	1265.0
MLLFC (m)	1870.0	1815.0
FZH (m)	3227.5	2855.0
FZH_W (m)	2832.5	2590.0
WS06 ($m\,s^{-1}$)	19.6	18.1
EBWD ($m\,s^{-1}$)	18.7	14.6
SRH01 ($m^2\,s^{-2}$)	34.3	31.4
SRH03 ($m^2\,s^{-2}$)	111.2	99.7

and MLCAPE are shown in Fig. 8a. Results show statistically significant differences between the distributions for SP-HAIL and SP-NONHAIL (Table 2). It is noteworthy that CAPE distributions follow positive skew distributions for SP-NONHAIL events, with the SP-HAIL median values being notably larger than SP-NONHAIL. However, the 25th percentile and median values for SP-HAIL SBCAPE, 758 and 1231 $J\,kg^{-1}$, respectively, are greater than those described by Kaltenböck et al. (2009) for Europe, approximately 400 and 1000 $J\,kg^{-1}$. According to Weisman and

Klemp (1982) and Markowski and Dotzek (2011), CAPE is dependent on humidity and orography, with slightly larger values in high elevations than in low terrains because potential temperature increases evenly with height. Therefore, the differences between the current study and the study by Kaltenböck et al. (2009) lie in the high elevations and relatively low humidity in the research area. The MLCAPE median value is close to the SBCAPE value and both also yield larger values for SP-HAIL than for SP-NONHAIL events. Kahraman et al. (2017) analyzed the convective storm environments for tornado and severe hail days from 1979 to 2013 in Turkey. In their study, severe thunderstorm environments are characterized by smaller CAPE when compared to the United States, highlighting that severe hail occurrence is associated with large CAPE and vertical WS. In the current analysis, the median values for MUCAPE, SBCAPE and MLCAPE (Table 3) in SP-HAIL events are slightly larger than those obtained by Kahraman et al. (2017) and Púčik et al. (2015) in their study of severe hail thunderstorms in central Europe. This discrepancy might be partially attributed to the warmer eastern surrounding seas (Mediterranean Sea and Black Sea; Shaltout and Omstedt, 2014) of the aforementioned studies. In the Taszarek et al. (2020b) study of severe convective thunderstorms with large hail, Europe MLCAPE median values are similar to those in the current study, with values around 1000 $J\,kg^{-1}$ for both. However, the US MLCAPE median value is 1200 $J\,kg^{-1}$. As discussed earlier, supercells in Europe tend to be smaller than those formed in the United States, with lower rotation values and shorter life cycles (Quirantes et al., 2014; Taszarek et al., 2020b). According to Rodriguez and Bech (2018), the CAPE values found
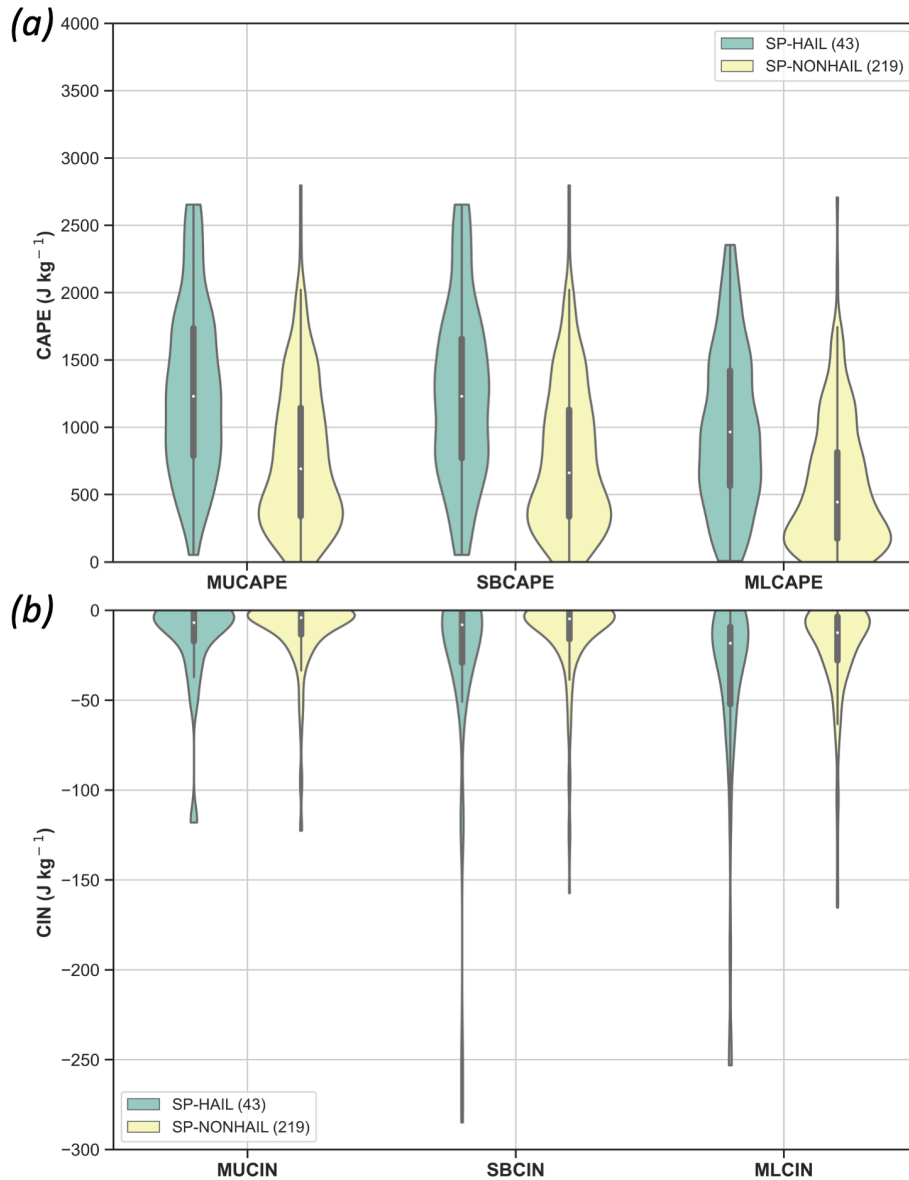
Figure 8. As in Fig. 7, but for **(a)** MUCAPE, SBCAPE and MLCAPE. **(b)** MUCIN, SBCIN and MLCIN.

in our study would correspond to those for tornadic storms in eastern Spain and the Balearic Islands. These authors analyzed a dataset of 907 tornadoes and waterspout events from 1980 to 2018 using atmospheric profiles from the ERA5 reanalysis and found SBCAPE values higher than $700\,\mathrm{J\,kg^{-1}}$ in tornadic storms (EF1 or stronger).

It is well known that due to limited vertical resolution, reanalyses do not represent capping inversions very well (Nevius and Evans, 2018; Coffer et al., 2020; Taszarek et al., 2021). Here, CIN distributions in the parcel measures MUCIN, SBCIN and MLCIN are displayed (Fig. 8b). The SP-HAIL and SP-NONHAIL differences for MLCIN distributions are statistically significant (Table 2). However, SBCIN and MUCIN differences are not statistically signif-

icant, presenting negative skew distributions for both events. The SP-HAIL events show a very weak inhibition layer (Fig. 8b) with an MLCIN median of $-20.2\,\mathrm{J\,kg^{-1}}$ (Table 3), and of $-12.2\,\mathrm{J\,kg^{-1}}$ for SP-NONHAIL. These values are slightly lower than those obtained by Taszarek et al. (2020b), who found MLCIN values of $-30\,\mathrm{J\,kg^{-1}}$ for large hail events in Central Europe. A stronger CIN may delay the convective initiation until the CAPE is maximized; once convection is triggered, discrete convective modes, including isolated and elevated supercells, can be developed producing large hail in the plains (Rasmussen and Blanchard, 1998; Smith et al., 2012; Thompson et al., 2012; Taszarek et al., 2020b). However, the CIN values in this survey are lower, probably due to the complex orography of the domain (Markowski and

Dotzek, 2011). Therefore, a mechanical lifting mechanism (e.g., air parcels lifted by orography or low-level convergence wind) is required to force convection initiation to overcome the LFC. The conjunction of these factors favors great vertical motions and organized convection.

A comparison of MLLCL, MLLFC, FZH and FZH_W percentiles and distributions between SP-HAIL and SP-NONHAIL is presented in Fig. 9. The MLLCL has been an important discriminator between tornadic and non-tornadic supercells in the United States (Rasmussen and Blanchard, 1998; Thompson et al., 2003). Taszarek et al. (2020b) compare the MLLCL in severe thunderstorms with hail greater than 5 cm in the United States and Europe obtaining great similarities between both continents. However, in Europe, the MLLCL tends to have much less variability in supercell events, and thus the skill of this indicator is limited (Kahraman et al., 2017; Taszarek et al., 2020b). The results shown here for Spain are in line with the previous conclusion, since there are no statistically significant differences (Table 2) for MLLCL between SP-HAIL and SP-NONHAIL events. Rodriguez and Bech (2018) also observed this low MLLCL variability between tornadic and non-tornadic thunderstorms in the Iberian Peninsula. Nevertheless, Púčik et al. (2015) obtained a MLLCL median value of 1000 m for severe hail thunderstorms in Central Europe, that matches those herein described for SP-HAIL events (Table 3). On the other hand, the MLLFC does not show significant differences between SP-HAIL and SP-NONHAIL (Table 2), with similar median values and variability. The MLLFC and MLLCL median values (Table 3) are also similar to those obtained by Taszarek et al. (2020b) for Europe. Another important factor for SP-HAIL and SP-NONHAIL events is the freezing level, with differences between both types of supercells being statistically significant for FZH and FZH_W (Table 2). Both FZH and FZH_W distributions for SP-NONHAIL events present higher variability than for SP-HAIL events (Fig. 9), with FZH and FZH_W median values for SP-HAIL being higher than for SP-NONHAIL (Table 3).

Several studies (Rasmussen and Blanchard, 1998; Púčik et al., 2015; Taszarek et al., 2019) suggest that the severity of the convective storms depend on the relationship between CAPE and WS. Furthermore, deep moist convection tends to develop more organized systems as the WS intensifies (Markowski and Richardson, 2011). WS between 0 and 6 km and EBWD distributions for SP-HAIL and SP-NONHAIL events are displayed in Fig. 10. As expected, the WS06 and EBWD values are higher for SP-HAIL than for SP-NONHAIL with statistically significant differences in EBWD (Table 2). The WS06 and EBWD median values for SP-HAIL (Table 3) match the results of Taszarek et al. (2020b) for severe convective storms with large hail in Europe; nevertheless, the values for the United States are higher than those presented here. Despite this, supercell events in the domain of study can be explained by the presence of several mountain ranges in the study area (Fig. 1) where the WS

is enhanced by the interaction between the wind field and orography, with a similar mechanism to the one observed in the Alps (Kunz et al., 2018; Taszarek et al., 2020b). However, ERA5 is limited in reproducing this enhancement due to its horizontal resolution.

Storm-relative helicity (SRH) is a frequent parameter used for forecasting supercells and tornadoes since it quantifies the streamwise vorticity that can support the development of rotating updrafts in right- and left-moving supercells (in this survey only the right-moving measure is used; Davies-Jones et al., 1990; Bunkers et al., 2002). Higher SRH values are usually related to the development of the mesocyclones and large hail formation (Rasmussen and Blanchard, 1998; Thompson et al., 2003). However, Hannesen et al. (1998), Kaltenböck (2004) and Gascón et al. (2015) suggested that complex orography such as in the current study domain can increase directional shear at low levels due to flow disturbance. Resulting large SRH03 values would produce favorable but not necessary conditions for severe thunderstorm formation. The SRH01 and SRH03 distributions (Fig. S2, Supplement) show no statistically significant differences (Table 2) between SP-HAIL and SP-NONHAIL. However, the SRH01 and SRH03 median values are slightly higher for SP-HAIL than for SP-NONHAIL (Table 3), showing similar variability. There are remarkable SRH03 90th percentile values for both groups of events, at $225 \, \text{m}^2 \, \text{s}^{-2}$, in line with the results of Kahmaran et al. (2017), who state that large hail occurrences are associated with large values of SRH03. Rodriguez and Bech (2018, 2021) obtained similar SRH03 values for EF0 and EF1 tornadoes and waterspouts in Iberia. The SRH03 results are also consistent with those reported by Calvo-Sancho (2021), where the SRH03 median spatial distribution in Spain displays values of almost $100 \, \text{m}^2 \, \text{s}^{-2}$ in the eastern half of Spain, and with the results of Taszarek et al. (2020b) in Europe for large hail reports.

4 Summary and conclusions

Here, the environments of SP-HAIL and SP-NONHAIL events are characterized and compared in Spain from 2011 to 2020. Different atmospheric variables are retrieved from the ERA5 reanalysis to obtain the synoptic patterns and composite soundings at the formation time of the supercells. Thermodynamic and kinematic parameters related to convective environments are also calculated and compared between SP-HAIL and SP-NONHAIL events.

The results yield several conclusions; the most important are listed below:

– There are notable differences in the spatial and monthly distributions of supercells in Spain. The eastern half of Spain accumulates 79.9 % of the SP-NONHAIL and 88.3 % of the SP-HAIL events. July and August accumulate 53.3 % of the SP-NONHAIL and 74.4 % of the
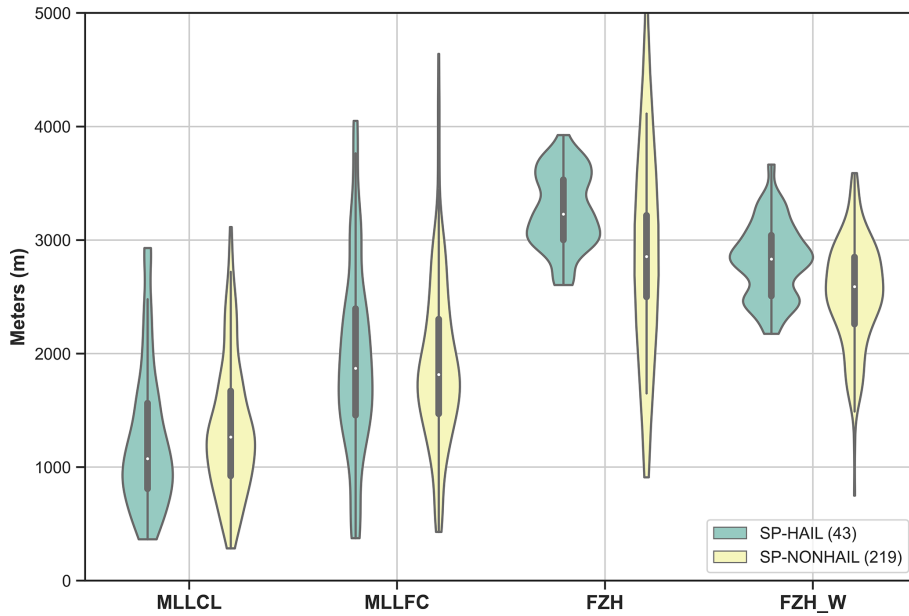
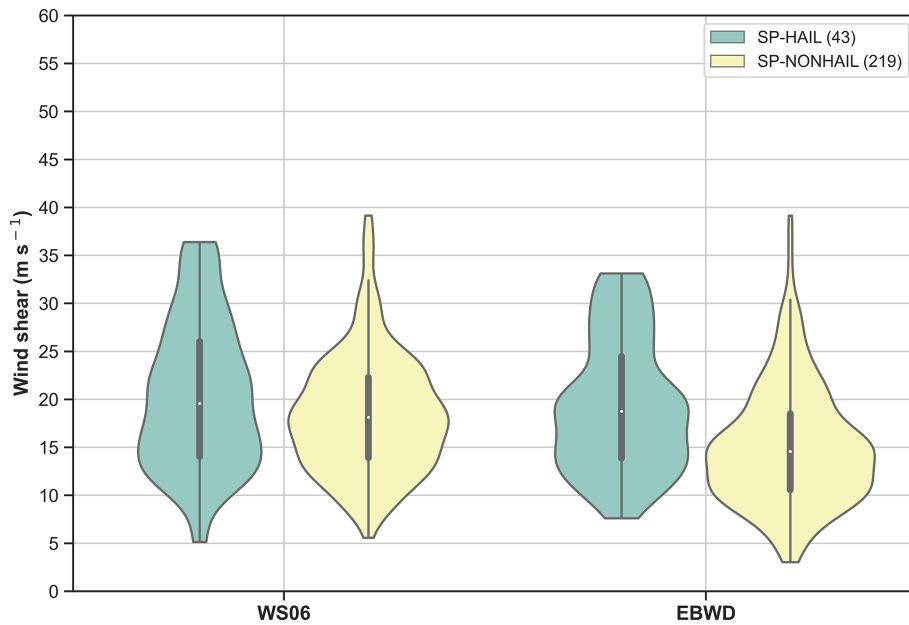**Figure 9.** As in Fig. 7, but for MLLCL, MLLFC, FZH and FZH_W.

Figure 10. As in Fig. 7, but for WS06 and EBWD.

SP-HAIL supercells. Most events are initiated between 12:00 and 19:00 UTC with a peak at 15:00 UTC.

- The synoptic pattern composites show a deeper trough for SP-NONHAIL in comparison with SP-HAIL composites at 500 hPa, with the largest height gradients corresponding to SP-HAIL. Strong upper-level forcing is promoted by vorticity advection and upper-level divergence. Surface humidity is influenced by the 10 m winds, being higher for SP-HAIL. The conjunction of these factors with wind convergences enables initiation of convection.

- The T2M and DWPT values are related to supercell monthly distributions with higher values corresponding to the warm season and minimum values to the cool season. Both variables are statistically different between SP-HAIL and SP-NONHAIL, with values being larger for the first group.

- Environments of SP-HAIL events are characterized by approximately 2 times larger MUCAPE median values than for SP-NONHAIL events. Moreover, higher CAPE, FZH and EBWD values and lower ML-CIN results are found for SP-HAIL compared with SP-NONHAIL. The differences for these parameters between both events are statistically significant at $p < 0.05$.

- Based on the ERA5 characterization results for SP-HAIL events in Spain, 75 % of the super-cells present $T2M > 21.1\,°C$, $DWPT > 12.0\,°C$, $MUCAPE > 781\,J\,kg^{-1}$, $MLCIN < -8.7\,J\,kg^{-1}$, $MLLFC > 1421\,m$, $FZH > 2986.3\,m$, $FZH\_W > 2497.5\,m$, $WS06 > 13.7\,m\,s^{-1}$ and $SRH03 > 74.7\,m^2\,s^{-2}$.

Finally, convective environments have been shown to be important factors to supercell formation and development. Thus, although ERA5 resolution improves previous reanalyses, more research is needed with high-resolution models, facilitating the study of the interactions between large-scale and convection processes in the genesis and development of hail supercell events. In addition, further research on the influence of orography in the genesis of supercells would be interesting.

Author contributions. CCS, JDF, YM, MLM, PB and JJGA designed the study. CCS and JDF performed the analysis and wrote the first manuscript. PB, JJGA, MS, and MLM supervised and reviewed the manuscript. DSM and JIF provided computational and software support. All authors discussed the results and edited the manuscript.

References

Antonescu, B., Schultz, D. M., Holzer, A., and Groenemeijer, P.: Tornadoes in Europe: An underestimated threat, B. Am. Meteorol. Soc., 98, 713–728, 2017.

Bedka, K., Murillo, E. M., Homeyer, C. R., Scarino, B., and Mersiovsky, H.: The above-anvil cirrus plume: An important severe weather indicator in visible and infrared satellite imagery, Weather Forecast., 33, 1159–1181, 2018.

Blair, S. F., Deroche, D. R., Boustead, J. M., Leighton, J. W., Barjenbruch, B. L., and Gargan, W. P.: A radar-based assessment of the detectability of giant hail, E-Journal of Severe Storms Meteorology, 6, 1–30, 2011.

Blair, S. F., Laflin, J. M., Cavanaugh, D. E., Sanders, K. J., Currens, S. R., Pullin, J. I., Cooper, D. T., and Mallinson, H. M.: High-resolution hail observations: Implications for NWS warning operations, Weather Forecast., 32, 1101–1119, 2017.

Bolgiani, P., Santos-Muñoz, D., Fernández-González, S., Sastre, M., Valero, F., and Martín, M. L.: Microburst detection with the WRF model: Effective resolution and forecasting indices, J. Geophys. Res.-Atmos., 125, e2020JD032883, https://doi.org/10.1029/2020JD032883, 2020.

Brooks, H. E., Lee, J. W., and Craven, J. P.: The spatial distribution of severe thunderstorm and tornado environments from global reanalysis data, Atmos. Res., 67, 73–94, 2003.

Brooks, H. E., Anderson, A. R., Riemann, K., Ebbers, I., and Flachs, H.: Climatological aspects of convective parameters from the NCAR/NCEP reanalysis, Atmos. Res., 83, 294–305, 2007.

Brooks, H. E., Doswell III, C. A., Zhang, X., Chernokulsky, A. A., Tochimoto, E., Hanstrum, B., Nascimento, E., Sills, D. M. L., Antonescu, B., and Barrett, B.: A century of progress in severe convective storm research and forecasting, Meteor. Mon., 59, 18.1–18.41, 2019.

Browning, K. A.: Cellular structure of convective storm, Meteorol. Mag., 91, 341–350, 1962.

Bunkers, M. J., Klimowski, B. A., and Zeitler, J. W.: The importance of parcel choice and the measure of vertical wind shear in evaluating the convective environment, Preprints, 21st Conf. Severe Local Storms, 11–16 August 2002, San Antonio, USA, American Meteorological Society, J117–J120, 11–16, https://ams.confex.com/ams/SLS_WAF_NWP/techprogram/paper_47319.htm (last access: 1 September 2022), 2002.

Calvo-Sancho, C.: Caracterización de los ambientes convectivos que favorecen el desarrollo de la convección organizada en España: exploración y evolución en el período 1979-2019 mediante reanálisis ERA5, Final Master Thesis, Universidad de Zaragoza, https://doi.org/10.13140/RG.2.2.25129.31841, 2021.

Calvo-Sancho, C. and Martín, Y.: Supercell Pre-convective Environments in Spain: a dynamic downscaling of ERA-5 Reanalysis, EGU General Assembly 2021, online, 19–30 April 2021, EGU21-2967, https://doi.org/10.5194/egusphere-egu21-2967, 2021.

Castro, A., Sánchez, J. L., and Fraile, R.: Statistical comparison of the properties of thunderstorms in different areas around the Ebro-Valley (Spain), Atmos. Res., 28, 237–257, 1992.

Chernokulsky, A., Kurgansky, M., Mokhov, I., Shikhov, A., Azhigov, I., Selezneva, E., Zakharchenko, D., Antonescu, B., and Kühne, T.: Tornadoes in northern Eurasia: From the middle age to the information era, Mon. Weather Rev., 148, 3081–3110, 2020.

Coffer, B. E., Taszarek, M., and Parker, M. D.: Near-Ground Wind Profiles of Tornadic and Nontornadic Environments in the United States and Europe from ERA5 Reanalyses, Weather Forecast., 35, 2621–2638, https://doi.org/10.1175/WAF-D-20-0153.1, 2020.

Consorcio de Compensación de Seguros: Estadística de Riesgos Extraordinarios, Serie 1971–220, http://www.consorseguros.es/web/documents/10184/44193/Estadistica_Riesgos_Extraordinarios_1971_2014/14ca6778-2081-4060-a86d-728d9a17c522 (last access: 30 January 2022), 2020.

Dahl, J. M. L.: Supercells – Their dynamics and prediction, MSc thesis, Dept. of Theoretical Meteorology, Free University of Berlin, 121 pp., http://www.estofex.org/files/dahl_thesis.pdf (last access: 28 June 2022), 2006.

Davenport, C. E.: Environmental Evolution of Long-Lived Supercell Thunderstorms in the Great Plains, Weather Forecast., 36, 2187–2209. 2021.

Davis-Jones, R., Burgess, D. W., and Foster, M.: Test of helicity as a forecast parameter. Preprints, 16th Conf. on Severe Local Storms, Kananaskis Park, AB, Canada, Amer. Meteor. Soc., 588–592, 1990.

Doswell III, C. A. and Rasmussen, E. N.: The effect of neglecting the virtual temperature correction on CAPE calculations, Weather Forecast., 9, 625–629, https://doi.org/10.1175/1520-0434(1994)009<0625:TEONTV>2.0.CO;2, 1994.

Dotzek, N., Groenemeijer, P., Feuerstein, B., and Holzer, A. M.: Overview of ESSL's severe convective storms research using the European Severe Weather Database ESWD, Atmos. Res., 93, 575–586, 2009.

Duda, J. D. and Gallus, W. A.: Spring and summer midwestern severe weather reports in supercells compared to other morphologies, Weather Forecast., 25, 190–206, https://doi.org/10.1175/2009WAF2222338.1, 2010.

Edwards, R., Allen, J. T., and Carbin, G. W.: Reliability and climatological impacts of convective wind estimations, J. Appl. Meteorol. Clim., 57, 1825–1845, 2018.

Elmore, K. L., Flamig, Z. L., Lakshmanan, V., Kaney, B. T., Farmer, V., Reeves, H. D., and Rothfusz, L. P.: mPING: Crowd-sourcing weather reports for research, B. Am. Meteorol. Soc., 95, 1335–1342, 2014.

Galanaki, E., Lagouvardos, K., Kotroni, V., Flaounas, E., and Argiriou, A.: Thunderstorm climatology in the Mediterranean using cloud-to-ground lightning observations, Atmos. Res., 207, 136–144, 2018.

García-Ortega, E., Merino, A., López, L., and Sánchez, J. L.: Role of mesoscale factors at the onset of deep convection on hailstorm days and their relation to the synoptic patterns, Atmos. Res., 114, 91–106, 2012.

Gascón, E., Merino, A., Sánchez, J. L., Fernández-González, S., García-Ortega, E., López, L., and Hermida, L.: Spatial distribution of thermodynamic conditions of severe storms in southwestern Europe, Atmos. Res., 164, 194–209, 2015.

Gatzen, C. P., Fink, A. H., Schultz, D. M., and Pinto, J. G.: An 18-year climatology of derechos in Germany, Nat. Hazards Earth Syst. Sci., 20, 1335–1351, https://doi.org/10.5194/nhess-20-1335-2020, 2020.

Gayà, M.: Tornadoes and severe storms in Spain, Atmos. Res., 100, 334–343, https://doi.org/10.1016/j.Atmosres.2010.10.019, 2011.

Gensini, V. A., Converse, C., Ashley, W. S., and Taszarek, M.: Machine Learning Classification of Significant Tornadoes and Hail in the United States Using ERA5 Proximity Soundings, Weather Forecast., 36, 2143–2160, 2021.

Groenemeijer, P., Púčik, T., Holzer, A. M., Antonescu, B., Riemann-Campe, K., Schultz, D. M., Kühne, T., Feuerstein, B., Brooks, H. E., Doswell III, C. A., Koppert, H. J., and Sausen, R.: Severe convective storms in Europe: Ten years of research and education at the European Severe Storms Laboratory, B. Am. Meteorol. Soc., 98, 2641–2651, 2017.

Gropp, M. E. and Davenport, C. E.: The impact of the nocturnal transition on the lifetime and evolution of supercell thunderstorms in the Great Plains, Weather Forecast., 33, 1045–1061, 2018.

Gutierrez, R. E. and Kumjian, M. R.: Environmental and Radar Characteristics of Gargantuan Hail–Producing Storms, Mon. Weather Rev., 149, 2523–2538, 2021.

Hannesen, R., Dotzek, N., Gysi, H., and Beheng, K. D.: Case study of a tornado in the Upper Rhine valley, Meteorol. Z., 7, 163–170, 1998.

Hersbach, H., Bell, B., Berrisford, P., Biavati, G., Horányi, A., Muñoz Sabater, J., Nicolas, J., Peubey, C., Radu, R., Rozum, I., Schepers, D., Simmons, A., Soci, C., Dee, D., and Thépaut, J.-N.: ERA5 hourly data on pressure levels from 1959 to present, Copernicus Climate Change Service (C3S) Climate Data Store (CDS) [data set], https://doi.org/10.24381/cds.bd0915c6, 2018.

Hersbach, H., Bell, B., Berrisford, P., Hirahara, S., Horányi, A., Muñoz-Sabater, J., Nicolas, J., Peubey, C., Radu, R., Schepers, D., Simmons, A., Soci, C., Abdalla, S., Abellan, X., Balsamo, G., Bechtold, P., Biavati, G., Bidlot, J., Bonavita, M., Chiara, G., Dahlgren, P., Dee, D., Diamantakis, M., Dragani, R., Flemming, J., Forbes, R., Fuentes, M., Geer, A., Haimberger, L., Healy, S., Hogan, R. J., Hólm, E., Janisková, M., Keeley, S., Laloyaux, P., Lopez, P., Lupu, C., Radnoti, G., Rosnay, P.,

Rozum, I., Vamborg, F., Villaume, S., and Thépaut, J.: The ERA5 global reanalysis, Q. J. R. Meteor. Soc., 146, 1999–2049, https://doi.org/10.1002/qj.3803, 2020.

Kahraman, A., Kadioglu, M., and Markowski, P. M.: Severe convective storm environments in Turkey, Mon. Weather Rev., 145, 4711–4725, 2017.

Kaltenböck, R.: The outbreak of severe storms along convergence lines northeast of the Alps. Case study of the 3 August 2001 mesoscale convective system with a pronounced bow echo, Atmos. Res., 70, 55–75, 2004.

Kaltenböck, R., Diendorfer, G., and Dotzek, N.: Evaluation of thunderstorm indices from ECMWF analyses, lightning data and severe storm reports, Atmos. Res., 93, 381–396, 2009.

Kotroni, V. and Lagouvardos, K.: Lightning in the Mediterranean and its relation with sea-surface temperature, Environ. Res. Lett., 11, 034006, https://doi.org/10.1088/1748-9326/11/3/034006, 2016.

Krennert, T., Pistotnik, G., Kaltenberger, R., and Csekits, C.: Crowdsourcing of weather observations at national meteorological and hydrological services in Europe, Adv. Sci. Res., 15, 71–76, https://doi.org/10.5194/asr-15-71-2018, 2018.

Kunz, M., Blahak, U., Handwerker, J., Schmidberger, M., Punge, H. J., Mohr, S., Fluck, E., and Bedka, K. M.: The severe hailstorm in southwest Germany on 28 July 2013: Characteristics, impacts and meteorological conditions, Q. J. Roy. Meteor. Soc., 144, 231–250, 2018.

Kunz, M., Wandel, J., Fluck, E., Baumstark, S., Mohr, S., and Schemm, S.: Ambient conditions prevailing during hail events in central Europe, Nat. Hazards Earth Syst. Sci., 20, 1867–1887, https://doi.org/10.5194/nhess-20-1867-2020, 2020.

Li, F., Chavas, D. R., Reed, K. A., and Dawson II, D. T.: Climatology of severe local storm environments and synoptic-scale features over North America in ERA5 reanalysis and CAM6 simulation, J. Climate, 33, 8339–8365, 2020.

López, L. and Sánchez, J. L.: Discriminant methods for radar detection of hail, Atmos. Res., 93, 358–368, 2009.

Mann, H. B. and Whitney, D. R.: On a test of whether one of two random variables is stochastically larger than the other, Ann. Math. Stat., 50–60, 1947.

Manzato, A.: Hail in northeast Italy: Climatology and bivariate analysis with the sounding-derived indices, J. Appl. Meteorol. Clim., 51, 449–467, 2012.

Markowski, P. and Richardson, Y.: Mesoscale meteorology in midlatitudes, vol. 2, John Wiley and Sons, ISBN 0470742135, 2011.

Markowski, P. M. and Dotzek, N.: A numerical study of the effects of orography on supercells, Atmos. Res., 100, 457–478, 2011.

Martín, Y., Cívica, M., and Pham, E.: Constructing a Supercell Database in Spain Using Publicly Available Two-Dimensional Radar Images and Citizen Science, Ann. Am. Assoc. Geogr., 111, 1346–1366, https://doi.org/10.1080/24694452.2020.1812371, 2020.

Melcón, P., Merino, A., Sánchez, J. L., López, L., and García-Ortega, E.: Spatial patterns of thermodynamic conditions of hailstorms in southwestern France, Atmos. Res., 189, 111–126, 2017.

Merino, A., García-Ortega, E., López, L., Sánchez, J. L., and Guerrero-Higueras, A. M.: Synoptic environment, mesoscale configurations and forecast parameters for hailstorms in Southwestern Europe, Atmos. Res., 122, 183–198, 2013.

Miglietta, M. M., Mazon, J. and Rotunno, R.: Numerical simulations of a tornadic supercell over the Mediterranean, Weather Forecast., 32, 1209–1226, https://doi.org/10.1175/WAF-D-16-0223.1, 2017.

Mohr, S., Kunz, M., Richter, A., and Ruck, B.: Statistical characteristics of convective wind gusts in Germany, Nat. Hazards Earth Syst. Sci., 17, 957–969, https://doi.org/10.5194/nhess-17-957-2017, 2017.

Mora, M., Riesco, J., de Pablo Dávila, F., and Rivas Soriano, L.: Atmospheric background associated with severe lightning thunderstorms in Central Spain, Int. J. Climatol., 35, 558–569, 2015.

Mulholland, J. P., Peters, J. M., and Morrison, H.: How does LCL height influence deep convective updraft width?, Geophys. Res. Lett., 48, e2021GL093316, https://doi.org/10.1029/2021GL093316, 2021.

National Weather Service (NWS): Supercell structure and dynamics, https://www.weather.gov/lmk/supercell/dynamics (last access: 24 January 2022), 2019.

Nevius, D. S. and Evans, C.: The influence of vertical advection discretization in the WRF-ARW Model on capping inversion representation in warm-season, thunderstorm-supporting environments, Weather Forecast., 33, 1639–1660, 2018.

Nisi, L., Martius, O., Hering, A., Kunz, M., and Germann, U.: Spatial and temporal distribution of hailstorms in the Alpine region: a long-term, high resolution, radar-based analysis, Q. J. Roy. Meteor. Soc., 142, 1590–1604, 2016.

Púčik, T., Groenemeijer, P., Rýva, D., and Kolář, M.: Proximity soundings of severe and nonsevere thunderstorms in central Europe, Mon. Weather Rev., 143, 4805–4821, 2015.

Quirantes Calvo, J. A., Riesco Martín, J., and Núñez Mora, J. Á.: Características básicas de las supercélulas en España, Agencia Estatal de Meteorología (AEMET), https://repositorio.aemet.es/bitstream/20.500.11765/709/10/Caracteristicas_supercelulas.pdf (last access: 28 June 2022), 2014.

Rasmussen, E. N. and Blanchard, D. O.: A baseline climatology of sounding-derived supercell and tornado forecast parameters, Weather Forecast., 13, 1148–1164, 1998.

Rodríguez, O. and Bech, J.: Sounding-derived parameters associated with tornadic storms in Catalonia, Int. J. Climatol., 38, 2400–2414, 2018.

Rodríguez, O. and Bech, J.: Tornadic environments in the Iberian Peninsula and the Balearic Islands based on ERA5 reanalysis, Int. J. Climatol., 41, E1959–E1979, 2021.

Romero, R., Ramis, C., Alonso, S., Doswell III, C. A., and Stensrud, D. J.: Mesoscale model simulations of three heavy precipitation events in the western Mediterranean region, Mon. Weather Rev., 126, 1859–1881, 1998.

Shaltout, M. and Omstedt, A.: Recent sea surface temperature trends and future scenarios for the Mediterranean Sea, Oceanologia, 56, 411–443, 2014.

Smith, B. T., Thompson, R. L., Grams, J. S., Broyles, C., and Brooks, H. E.: Convective modes for significant severe thunderstorms in the contiguous United States. Part I: Storm classification and climatology, Weather Forecast., 27, 1114–1135, 2012.

Taszarek, M., Brooks, H. E., and Czernecki, B.: Sounding-derived parameters associated with convective hazards in Europe, Mon. Weather Rev., 145, 1511–1528, 2017.

Taszarek, M., Brooks, H. E., Czernecki, B., Szuster, P., and Fortuniak, K.: Climatological aspects of convective parameters

over Europe: A comparison of ERA-interim and sounding data, J. Climate, 31, 4281–4308, https://doi.org/10.1175/JCLI-D-17-0596.1, 2018.

Taszarek, M., Allen, J., Púčik, T., Groenemeijer, P., Czernecki, B., Kolendowicz, L., Lagouvardos, K., Kotroni, V., and Schulz, W.: A climatology of thunderstorms across Europe from a synthesis of multiple data sources, J. Climate, 32, 1813–1837, https://doi.org/10.1175/JCLI-D-18-0372.1, 2019.

Taszarek, M., Allen, J. T., Groenemeijer, P., Edwards, R., Brooks, H. E., Chmielewski, V., and Enno, S. E.: Severe convective storms across Europe and the United States. Part I: Climatology of lightning, large hail, severe wind, and tornadoes, J. Climate, 33, 10239–10261, https://doi.org/10.1175/JCLI-D-20-0345.1, 2020a.

Taszarek, M., Allen, J. T., Púčik, T., Hoogewind, K. A., and Brooks, H. E.: Severe Convective Storms across Europe and the United States. Part II: ERA5 Environments Associated with Lightning, Large Hail, Severe Wind, and Tornadoes, J. Climate 33, 10263–10286, https://doi.org/10.1175/JCLI-D-20-0346.1, 2020b.

Taszarek, M., Pilguj, N., Allen, J. T., Gensini, V., Brooks, H. E., and Szuster, P.: Comparison of convective parameters derived from ERA5 and MERRA-2 with Rawinsonde data over Europe and North America, J. Climate, 34, 3211–3237, 2021.

Thompson, R. L., Edwards, R., Hart, J. A., Elmore, K. L., and Markowski, P.: Close proximity soundings within supercell environments obtained from the Rapid Update Cycle, Weather Forecast., 18, 1243–1261, 2003.

Thompson, R. L., Mead, C. M., and Edwards, R.: Effective storm-relative helicity and bulk shear in supercell thunderstorm environments, Weather Forecast., 22, 102–115, 2007.

Thompson, R. L., Smith, B. T., Grams, J. S., Dean, A. R., and Broyles, C.: Convective modes for significant severe thunderstorms in the contiguous United States. Part II: Supercell and QLCS tornado environments, Weather Forecast., 27, 1136–1154, 2012.

Tomas-Burguera, M., Beguería, S., and Vicente-Serrano, S. M.: Climatology and trends of reference evapotranspiration in Spain, Int. J. Climatol., 41, E1860–E1874, 2021.

Tullot, I. F.: Climatología de España y Portugal, vol. 76, Universidad de Salamanca, ISBN 8478009442, 2000.

Vicente-Serrano, S. M., Azorin-Molina, C., Sanchez-Lorenzo, A., Revuelto, J., López-Moreno, J. I., González-Hidalgo, J. C., Moran-Tejeda, E., and Espejo, F.: Reference evapotranspiration variability and trends in Spain, 1961–2011, Global Planet. Change, 121, 26–40, 2014.

Weisman, M. L. and Klemp, J. B.: The dependence of numerically simulated convective storms on vertical wind shear and buoyancy, Mon. Weather Rev., 110, 504–520, 1982.

Westermayer, A., Púčik, T., Groenemeijer, P., and Tijssen, L.: Comparison of sounding observations and reanalysis of thunderstorm environments, Eighth European Conf. on Severe Storms, 14–18 September 2015, Wiener Neustadt, Austria, European Severe Storms Laboratory, http://meetingorganizer.copernicus.org/ECSS2015/ECSS2015-136-1.pdf (last access: 28 June 2022), 2016.